RESEARCH ARTICLE | OCTOBER 02 2024

Predicting p53-dependent cell transitions from thermodynamic models

Special Collection: Chromatin Structure and Dynamics: Recent Advancements

Pankaj Gautam ; Isabella Ciuta ; Vladimir B. Teif ; Sudipta Kumar Sinha

J. Chem. Phys. 161, 135101 (2024)
https://doi.org/10.1063/5.0225166

The Journal of Chemical Physics ARTICLE pubs.aip.org/aip/jcp

Predicting p53-dependent cell transitions from thermodynamic models

Cite as: J. Chem. Phys. 161, 135101 (2024); doi: 10.1063/5.0225166
Submitted: 23 June 2024 • Accepted: 18 September 2024 •
Published Online: 2 October 2024

Pankaj Gautam,[1] Isabella Ciuta,[2] Vladimir B. Teif,[2,a)] and Sudipta Kumar Sinha[1,a)]

AFFILIATIONS

[1] Theoretical and Computational Biophysical Chemistry Group, Department of Chemistry, Indian Institute of Technology Ropar, Rupnagar, Punjab 140001, India

[2] School of Life Sciences, University of Essex, Wivenhoe Park, Colchester CO4 3SQ, United Kingdom

Note: This paper is part of the JCP Special Topic on Chromatin Structure and Dynamics: Recent Advancements.
[a)]**Authors to whom correspondence should be addressed:** vteif@essex.ac.uk and sudipta@iitrpr.ac.in

ABSTRACT

A cell's fate involves transitions among its various states, each defined by a distinct gene expression profile governed by the topology of gene regulatory networks, which are affected by 3D genome organization. Here, we develop thermodynamic models to determine the fate of a malignant cell as governed by the tumor suppressor p53 signaling network, taking into account long-range chromatin interactions in the mean-field approximation. The tumor suppressor p53 responds to stress by selectively triggering one of the potential transcription programs that influence many layers of cell signaling. These range from p53 phosphorylation to modulation of its DNA binding affinity, phase separation phenomena, and internal connectivity among cell fate genes. We use the minimum free energy of the system as a fundamental property of biological networks that influences the connection between the gene network topology and the state of the cell. We constructed models based on network topology and equilibrium thermodynamics. Our modeling shows that the binding of phosphorylated p53 to promoters of target genes can have properties of a first order phase transition. We apply our model to cancer cell lines ranging from breast cancer (MCF-7), colon cancer (HCT116), and leukemia (K562), with each one characterized by a specific network topology that determines the cell fate. Our results clarify the biological relevance of these mechanisms and suggest that they represent flexible network designs for switching between developmental decisions.

I. INTRODUCTION

The p53 tumor suppressor protein regulates the expression of a large number of genes in response to DNA damage.[1,2] Such changes in gene expression are responsible for determining cell differentiation and many processes such as cell cycle, DNA damage repair, and apoptosis.[3,4] The p53-signalling pathway is critical for controlling checkpoints in cell division and suppressing tumorigenesis. Perturbations in the pathway could compromise p53 activity and consequently promote tumor development.

Genotoxic stress created by DNA damage increases the transcriptional activity of p53. Unstressed cells maintain low levels of p53 by continuous proteasomal degradation mediated by a protein MDM2.[5,6] On the other hand, genome damage initiates cascades of phosphorylation and acetylation to sustain and stabilize the amount of p53, which may lead to cell cycle arrest and apoptosis.[7,8] Post-translational modifications of p53 regulate its transcriptional activity, which affects the action of its binding partners. Recently, it has been demonstrated that p53 activation drives dramatic genome-wide changes in 3D genome organization to trigger a temporally dependent transcriptional response against cellular stress.[9] This leads to extensive rewiring of p53-bound enhancer-promoter loops.[9] It has been also proposed that p53 action may be affected by its self-assembly through phase separation,[10,11] but mathematical models of such effects in relation to gene network rewiring are missing.

Multiple studies suggest that the degree of phosphorylation of p53 significantly affects its binding affinity with DNA. Single-site phosphorylation of p53 at Thr18 results in a twofold increase in affinity to DNA; double-site phosphorylation at Ser15 and Thr18 leads to an approximately fivefold increase; and triple-site phosphorylation at Ser15, Thr18, and Ser20 causes more than ten-fold increase in binding affinity to DNA.[12,13] The degree of

phosphorylation can affect phenotypical changes of a cell and cancer progression.[12,14] This has been verified in murine cells, where single-site phosphorylation of serine or threonine of p53 has little effect, but their simultaneous phosphorylation has a more significant effect, indicating that multisite phosphorylation acts synergistically.[12,15] In human cells, simultaneous phosphorylation of threonine and serine is also synergistic, increasing p53 responses.[16,17] However, the mechanism linked with phosphorylation and especially multisite phosphorylation in controlling p53 activation remains unclear.[8,14]

Under stressed conditions, cells produce an increased amount of p53 that may not degrade during the cell cycle. The excess p53 undergoes phosphorylation upon the action of external stimuli, leading to a series of transcriptional activation processes.[15,18] In our analysis, we investigate how cellular processes, such as cell cycle arrest, DNA repair, inhibition of angiogenesis, and apoptosis,[19,20] are governed by the binding of phosphorylated tetramers of p53 (denoted as p53*) to the promoter regions of the minimalist network of four genes: P21,[21] P48,[22] PAI,[23] and BAX.[15,24] These four genes are among many genes regulated by p53, and while they do not constitute a closed system, we have selected them as representative players of the processes mentioned above to study the conceptual possibility of rewiring of the p53 network. Even the interactions between these few players are quite complex. Upon p53 activation, expression of P21 promotes cell-cycle arrest; P48 activates DNA repair; PAI suppresses tumor angiogenesis; and BAX promotes apoptosis. Recent studies have shown that these cell-fate-determining genes follow a concerted path as they are influenced by each other through protein–protein interactions or contacts.[25,26] Their interconnections vary for different stimuli and cancer cell types, as exemplified by p21-dependent activation of BAX-gene leading to apoptosis in MCF-7 but p21-dependent prevention of apoptosis in HCT116.[27,28] The mechanism behind p21-dependent apoptosis is still unclear, but it is believed that phosphorylated p53 promotes the production of p21 protein that binds the CDK–cyclin complex.[29–31] High levels of p21 expression result in cell cycle arrest and promote apoptosis in a p53-dependent manner.[25,32] Moreover, p21 is also known for regulating a number of other genes that cause inhibition of angiogenesis and DNA repair.[33,34] Other important players in this system are PAI, P48, and BAX, which also act as regulators of apoptosis.[35]

Differential binding of a phosphorylated p53 tetramer to the response elements of the cell fate-determining genes modulates gene expression and consequently determines the state of a cell. Moreover, various cancer cell lines may have different internal gene regulatory networks connecting these four genes, further introducing differences in gene expression that affect the cell fate.[28,36,37]

The mechanism behind p53-mediated regulation is complex and requires a system-level analysis.[8,38] However, a minimal regulatory network model can be constructed based on four cell-fate determining genes for this system, presented in Fig. 1. This model considers how the cell under stress can promote a phase transition between free promoter/bound promoter states upon binding of p53* to the promoter regions of the four cell fate-determining genes, BAX, P21, P48, and PAI. The p53 gene transcribes p53 proteins, which then undergo degradation under normal conditions.[39] The p53 proteins activate the MDM2 gene that produces the MDM2 protein, which promotes p53 degradation under normal conditions. The unphosphorylated MDM2 interacts with p53, which promotes

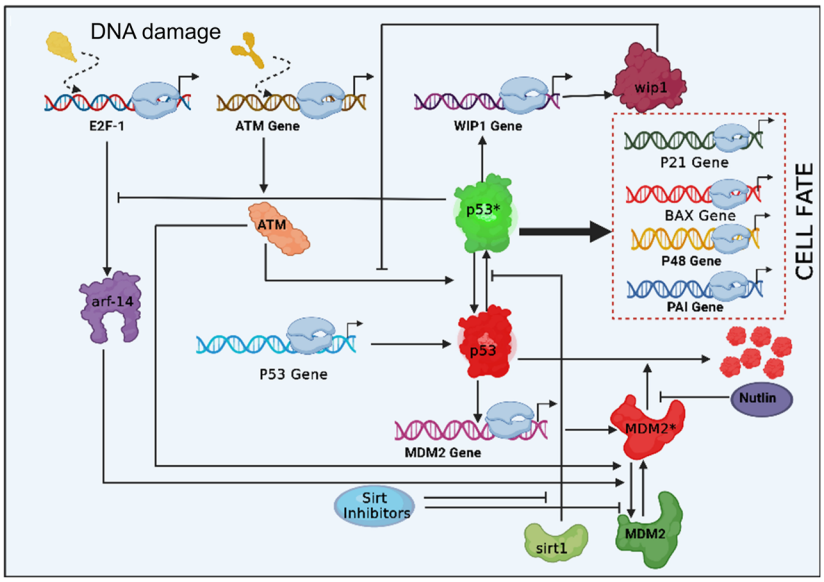

FIG. 1. A scheme showing a minimalistic model of the cell response to environmental stress within the p53-mediated signaling pathway. The stress triggers cascading events ranging from DNA damage to the production of phosphorylated p53 (p53*). p53* and p53 bind competitively to the promoter regions of four cell fate-determining genes as shown in the dotted box. The network connectivity among the cell fate genes may be different in different cells. The relative populations of the products of these genes determine the fate of a cell.

its degradation, thereby forming a negative feedback loop.[40] However, the population of p53 is significantly enhanced if the cell is under stress. The excess p53 undergoes phosphorylation by ATM that controls the fractions of p53* and p53. p53* inhibits binding to MDM2 but promotes the binding with the promoter region of cell fate genes.[18,41]

A small molecule Nutlin can be used to inhibit p53-MDM2 interactions. Nutiln binds to MDM2, preventing MDM2 binding to p53 and thus inhibiting the MDM2-dependent degradation of p53.[42,43] Phosphorylated p53 simultaneously activates WIP and miR genes, producing WIP1 protein and small RNA, miR-16. The WIP1 protein inhibits the formation of phosphorylated p53, while miR-16 further inhibits the production of the WIP1 protein. The phosphorylated p53 binds to the promoter region of four genes, BAX, P21, P48, and PAI, controlling a cell's fate.[4,44]

The interconnections between these four cell fate-determining genes may vary in different cells. Therefore, we will consider three cancer cell lines: (a) breast cancer (MCF-7), (b) colorectal cancer (HCT116), and (c) leukemia (K562) to compare their p53-dependent regulation.[27,28,45–50] The network topology among the genes of these three cell lines is different, resulting in different gene expression patterns and determining the cell fate.[36,37] In MCF-7, p21 has been shown to activate both P48 and BAX genes along with facilitating the binding of p53* to the promoter regions of the four genes.[27,45] This leads to cell cycle arrest and induces apoptosis in a drug-dependent manner.[51] In the case of HCT116 cells, p21 represses both p48 and BAX genes.[28,46] However, p21 activates p48 and represses BAX in K562 cells.[36,47,50] Such differences in interconnectivity among the genes result in differential gene expression that affects these cancer cells differently.

In this work, we aim to explore the following crucial questions: (a) Does a cell undergo a phase transition between different states upon p53* binding? (b) How do the differences in the network topologies for different cancer cell lines (MCF-7, HCT116, K562) define their different gene expression patterns? To address the first question, we constructed an equilibrium thermodynamic model, taking into account long-range chromatin interactions in the mean-field approximation. To address the second question, we constructed a network model of this system. Our analysis reveals that the differential gene expression that defines a cell's fate is strongly modulated by the topologies of gene networks and the free energy of protein–DNA and protein–protein binding.

II. METHODS

We use two independent methods to describe the organization of proteins on the DNA lattice and their effect on gene expression for determining the cell fate. In the first method, we follow a minimum free energy method considering short- and long-range interactions between DNA-bound proteins. The second method uses a grand canonical partition function of an interaction network-based statistical thermodynamic approach. The first method does not consider the network's topology, while the second method explicitly considers the network's topology. We analyze both models in Secs. II A and II B. Our proposed models are general and can be extended for any arbitrary number of promoters.

A. The free energy minimum method to calculate equilibrium DNA-transcription factor binding

Here, we adopt the free energy minimum method for equilibrium protein binding to gene promoter regions in a large DNA molecule in solution.[52,53] Our model treats DNA as a one-dimensional lattice containing N lattice units that can bind p53. p53 molecules can be either free in solution at concentration c_0 or bound to DNA. Let there be a total of k DNA-bound p53 proteins in the system. Let m be the number of DNA lattice units covered by p53 upon DNA binding, b be the number of contacts between DNA-bound proteins, and σ be the number of phosphorylated p53 molecules. To account for all possible rearrangements for the binding of proteins on the DNA lattice, we use a free energy function, $F(k,b,\sigma)$. Both unphosphorylated p53 and phosphorylated (p53*) molecules can bind specifically to their binding sites on the DNA or reside free in solution. Then, the free energy is defined as follows:[52,53]

$$F(k,b,\sigma) = k\cdot\varepsilon_0 - k\cdot g(k) + b\cdot\varepsilon_1 + \sigma\cdot\varepsilon_2 - R\cdot T\cdot\log(W). \quad (1)$$

Here, the first term accounts for the free energy (ε_0) of direct binding of k molecules of p53 to DNA.

The second term, $k\cdot g(k)$, is associated with the free energy of long-range interactions between k DNA-bound proteins in the mean-field approximation. Such an interaction may originate from changes in 3D genome organization (chromatin fiber packing/compartmentalization/DNA looping, etc.), which may also alter the topology of the protein–DNA interaction network. Since we have considered all bound proteins interacting with each other, it is reasonable to assume that g is a function of the number of bound protein molecules on the DNA, k. Note that direct contact interactions between DNA-bound proteins are not included here and accounted for in a separate term in Eq. (1) (Fig. 2). We use the simplest linear form of the potential of long-range interactions $g(k) = w\cdot c$ (per bound protein), where c is the relative degree of protein binding, $c = k/N$. This linear form of potential has been previously used to describe the binding of ligands and metal ions to DNA.[52,53] Historically, such a long-range interaction

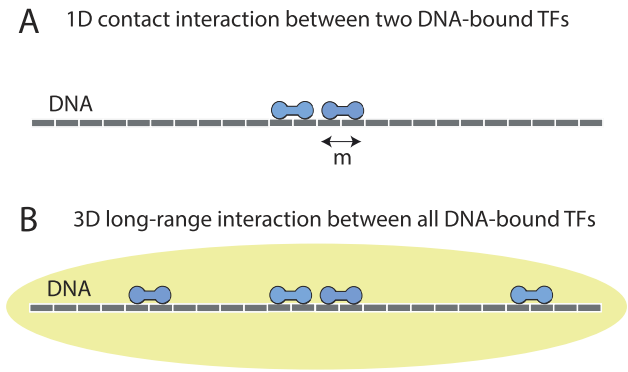

FIG. 2. A scheme of the lattice models for 1D contact interactions between neighboring DNA-bound proteins (a) and 3D long-range interactions between all DNA-bound proteins (b). The latter term, quantified as a function $g(k)$, takes into account the changes in the chromatin organization due to p53 binding.

potential, which depends on the number of biopolymer-bound ligands, goes back to the works of Scatchard, where it had a purely electrostatic nature.[54]

In the third term, we include the contact interactions $(b \cdot \varepsilon_1)$ between bound p53 molecules on the DNA lattice (Fig. 2). Here, b is the number of pairwise contacts between DNA-bound proteins. The free energy associated with each contact is ε_1. The values of b lie within the interval $0 \le b \le k-1$ if $0 < k \le N/(m+1)$ and $(m+1)k - N - 1 \le b \le k-1$ if $N/(m+1) < k \le N/m$.

The fourth term accounts for the phosphorylation of p53. A few of the p53 residues, such as threonine or serine, may undergo phosphorylation. We consider that σ p53 molecules undergo phosphorylation among a total of k DNA-bound p53 molecules. Each phosphorylated p53* contributes additional ε_2 free energy for binding to DNA. The value of σ lies in the interval $0 \le \sigma \le k$.

The fifth term is associated with the entropy contribution due to the number of ways to arrange k p53 molecules that form b p53–p53 contacts on the DNA lattice of size N. One can calculate this combinatorial factor W as follows:

$$W = \frac{(N - m\cdot k)!}{[N-(m+1)\cdot k + b)]!(k-1-b)!} \cdot \frac{(k-1)!}{(k-1-b)!b!} \cdot \frac{k!}{(k-\sigma)!\sigma!}. \tag{2}$$

For simplicity, we chose $m = 2$ for our calculation, assuming that a binding site of a p53 tetramer consists of two equal halves; another protein cannot bind to the same m lattice units. If the concentration of p53 in the cell nucleus is c_0, the change in free energy upon DNA binding of k proteins that have σ phosphorylated sites and form b contacts between proteins that occupy adjacent base pairs may be written as

$$\Delta F(k,b,\sigma) = F(k,b,\sigma) - k\cdot[\mu_0 + R\cdot T\cdot \log(c_0)]. \tag{3}$$

The last term in this equation is the loss of free energy due to the removal of k p53 molecules from the solution upon their binding to DNA. Here, the chemical potential of p53 in solution is $\mu = \mu_0 + R\cdot T\cdot\log(c_0)$, where μ and μ_0 are the chemical potentials of the p53 in solution and its standard state and R and T are the gas constant and absolute temperature.

Once we define the free energy function for the protein–DNA binding, we can optimize it to obtain its equilibrium properties. Following the previous works,[52,53] we apply the Stirling approximation assuming large values of k, b, σ, and N to obtain their most probable or the equilibrium values k^* or $c^* = k^*/N$, b^*, and σ^*,

$$\exp\left(\frac{\mu_0-\varepsilon_0}{RT}\right)\cdot\exp\left(\frac{2wc^*}{RT}\right) = \frac{(1-mc^*)^m}{1-(m+1)c^*+z_1} \times \frac{(c^*-z_1)^2}{c^*}\frac{(c^*-z_2)}{c_0c^*}, \tag{4}$$

$$\exp\left(-\frac{\varepsilon_1}{RT}\right) = (1-(m+1)c^*+z_1)\frac{z_1}{(c^*-z_1)^2}, \tag{5}$$

$$\exp\left(-\frac{\varepsilon_2}{RT}\right) = \frac{z_2}{(c^*-z_2)}. \tag{6}$$

Here, $K = \exp\left(\frac{\mu_0-\varepsilon_0}{RT}\right)$ is the binding constant, $A(c^*) = \exp\left(\frac{2wc^*}{RT}\right)$ is the cooperativity parameter related to long-range interactions, $a_1 = \exp\left(-\frac{\varepsilon_1}{RT}\right)$ is the contact cooperativity parameter for interactions of DNA-bound proteins, and $a_2 = \exp\left(-\frac{\varepsilon_2}{RT}\right)$ is the cooperativity parameter accounting for differential phosphorylation of p53. $z_1 = b^*/N$ is the relative concentration of ligand–ligand contacts and $z_2 = \sigma^*/N$ is the relative phosphorylation. Equations (4)–(6) are solved simultaneously and then combined with Eq. (3) to define $\Delta F(c^*, b^*, \sigma^*)$ for a given c_0,

$$\begin{aligned}\frac{\Delta F^*}{NRT} = &-c^*\log(K\cdot B^*\cdot c_0\cdot(c^*)^2) - z_1\log(a_1) - z_2\log(a_2)\\ &-(1-mc^*)\cdot\log(1-m\cdot c^*) + 2(c^*-z_1)\log(c^*-z_1)\\ &+(c^*-z_2)\log(c^*-z_2) + z_1\log(z_1) + z_2\log(z_2)\\ &+(1-(m+1)c^*+z_1)\log(1-(m+1)c^*+z_1),\end{aligned}$$

where $B^* = \exp(G(c^*)/RT) = \exp(wc^*/RT)$.

Note that the model above addresses a specific question, and for simplicity, it does not consider different classes of binding sites and different types of transcription factors (apart from the fact that p53 can be phosphorylated or not), but it is straightforward to generalize it to sequence-specific combinatorial cooperative binding of multiple proteins, as in our previous publication.[55]

B. Grand partition function for the gene network

A gene regulatory network (GRN) is a directed graph determining the cell fate. The elements of this graph are proteins or transcription factors and the promoters of the genes. The proteins can bind to the promoter regions of the target genes, and the genes can interact with each other if proteins occupy their promoter sites. In our system, four genes, p21, p48, PAI, BAX, and protein p53* constitute a small network. The phosphorylated p53* binds to the promoter region of these four genes, and there is an interaction among the genes. In particular, one can realize the protein occupancy-dependent directed interaction if proteins occupy both participating promoters. We further assume that RNA polymerase (RNAP) is present in the system at saturation. The network wiring is critical because it can vary for different cell lines,[36,37] defining different cell fates.

We define the network as a directed graph (G), where we consider promoters of the genes as vertices (V) where a protein can bind specifically, and the protein–promoter and promoter–promoter interactions form the edges (E). In particular, one can realize the protein occupancy-dependent edges if proteins occupy both participating promoters. Depending on their binding, one can realize the existence of a set of such directed graphs or an ensemble of configurations of such a network. We aim to measure the expectation of occupation numbers of proteins as observable $(\langle s\rangle)$ from the G. In order to measure such a quantity, we calculate the probability of a specific configuration, $P(G)$, so that the expectation value of the observable within the ensemble is equal to the observed value. With this in mind, we can define the Hamiltonian of the network as follows:

$$H(G) = \sum_i \sum_{s_i=0}^{1} \varepsilon_i s_i + \sum_{i\neq j}\sum_{\sigma_{ij}=0}^{1}\omega_{ij}\sigma_{ij}. \tag{7}$$

Here, the symbol G within the parentheses of the Hamiltonian is used to define the topology of the directed graph, and ε_i and ω_{ij} are the free energy of protein–DNA and promoter–promoter interactions, respectively; s_i takes a value of 1 if there exists a direct protein–DNA interaction; otherwise, it takes value 0. We assume

that there is a total of M such binding sites in the network. σ_{ij} is the adjacency matrix for the interaction among genes, which takes a value of either 1 or 0 depending on connections. Note that σ_{ij} is not symmetric in our model, which may be true in general for a real gene regulatory network. The topology of the graph (G) is replaced by the specific protein–DNA (s_i) and promoter–promoter interactions (σ_{ij}) in the Hamiltonian. According to our model, the free energy of interaction of the RNAP with the promoter depends on the values

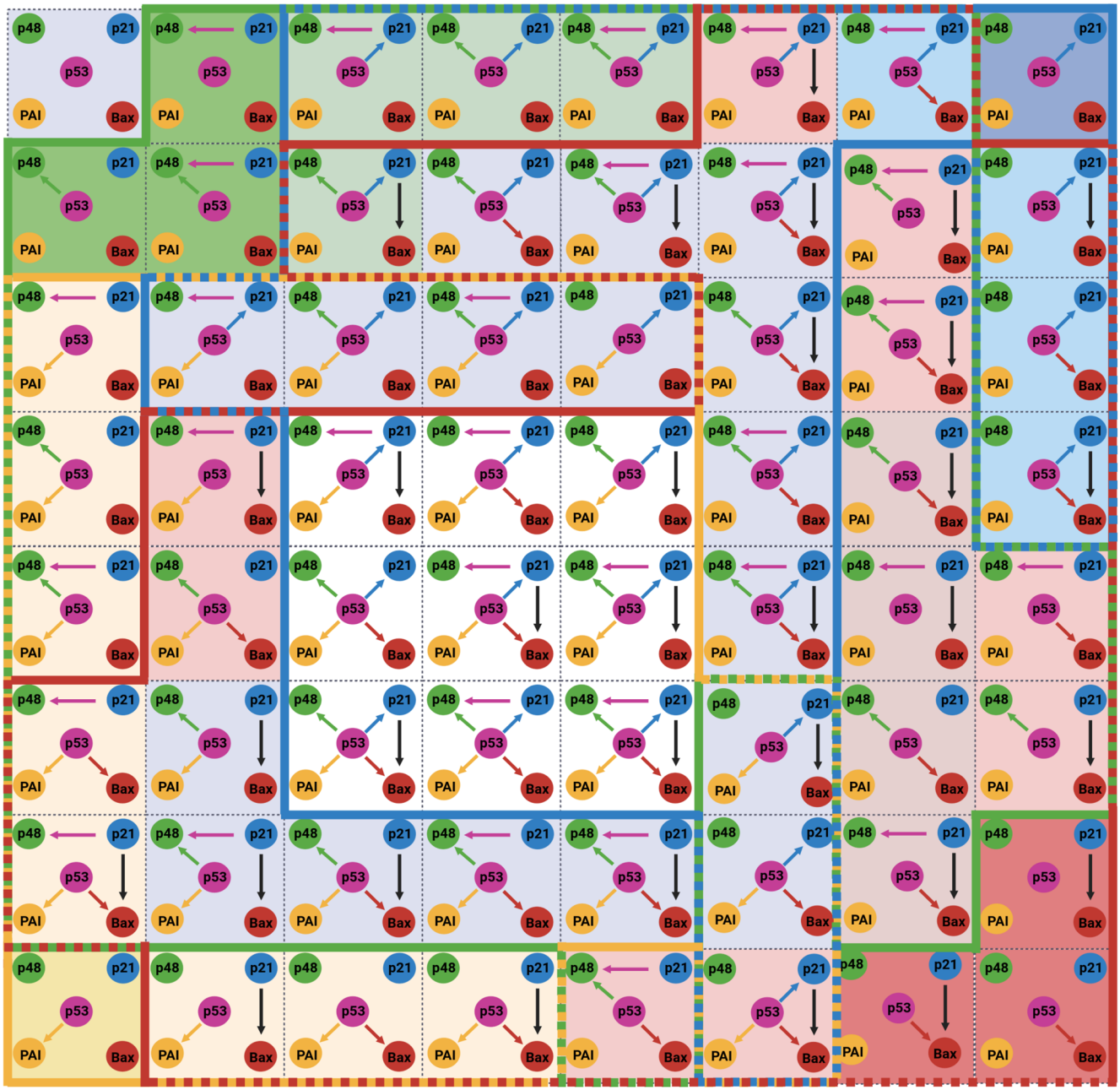

FIG. 3. A scheme demonstrating all 64 possible microstates for the gene regulatory network of the MCF-7 breast cancer cell line. We marked with green, blue, yellow, and red background color regions for the configurations associated with cell fate genes, P48, P21, PAI, and BAX, respectively. The solid and shed backgrounds are used to show the exclusive and shared configurations for a specific gene. Similarly, the solid and dashed lines of different colors are used to show the border for a specific gene's exclusive and shared configurations. The configurations located at the middle white background region are common to all genes.

of σ_{ij} and the type of interaction. We emphasize the type of interaction between protein and promoter or protein-mediated interactions among promoters, which are specific as they often act as activators or repressors toward a specific gene. However, that protein may not be an activator or a repressor for other genes in general. We incorporate these facts into our model: (a) if a protein acts as an activator, the RNAP binding to the promoter strengthens. (b) However, if it is a repressor, the RNAP binding to the promoter weakens and is finally replaced by the repressor. If the total no of proteins is N, then $\sum_i s_i = N$. If we assume s_i and σ_{ij} are independent, then the Grand partition function for a network is

$$\begin{aligned}\Xi &= \sum_{N=0}^{\infty}\sum_{G}\exp\left(-\beta H(G)\right)\lambda^{N}\\ &= \sum_{N=0}^{\infty}\sum_{G}\exp\left(-\beta\left(\sum_{i}\sum_{s_i=0}^{1}\varepsilon_i s_i+\sum_{i\neq j}\sum_{\sigma_{ij}=0}^{1}\omega_{ij}\sigma_{ij}\right)\right)\lambda^{\sum_i s_i}\\ &= \sum_{\{s_i,\sigma_{ij}\}}\exp\left(-\beta\left(\sum_{i}\sum_{s_i=0}^{1}\varepsilon_i s_i\right)\right)\lambda^{s_i}\exp\left(-\beta\sum_{\sigma_{ij}=0}^{1}\omega_{ij}\sigma_{ij}\right)\\ &= \prod_{i}\left(1+\lambda\exp\left(-\beta\varepsilon_i\right)\right)\prod_{i\neq j}\left(1+\exp\left(-\beta\omega_{ij}\right)\right),\end{aligned}$$

where λ is the $\exp(\beta\mu)$ and μ is the chemical potential of p53* and β is the inverse of thermal energy, $k_B T$. There are M terms in the first product and $M(M-1)$ terms in the second product, respectively. One can calculate the average occupancy of p53* on each of the genes by taking

$$\langle s\rangle = \frac{\lambda}{M}\left(\frac{\partial \ln\Xi}{\partial\lambda}\right)_{T,M} = \frac{\sum_{i=1}^{N}\lambda\exp\left(-\beta\varepsilon_i\right)}{\Xi} \tag{8}$$

We express our results by the fold change (FC), defined as the normalized protein's occupancy relative to its basal value. However, in practice, genes are influenced by each other through protein–protein interaction, which immediately restricts the application of the independence between s_i and σ_{ij}. To explore all the effects together, we first list all possible network configurations, as shown in Fig. 3. We then identify all the configurations where at least one p53* is bound to a particular promoter. The ratio of statistical weights between those configurations and the total number of configurations provides a signature of the probability of gene expression of that particular gene. Note that the counting process becomes exceedingly complex as the network size increases. Therefore, one can employ Monte Carlo (MC) simulations that offer an elegant approach to identifying those relevant configurations for expressing a particular gene in a large network for a given set of binding parameters.[56–58] The networks can be constructed based on a number of previous publications (Table I). We estimate the parameters ε_i and ω_{ij} from ChIP-seq experiments, where we analyzed a binding profile of phosphorylated p53 by calculating the occupancy of phosphorylated p53* genome-wide in the MCF-7 cancer cell line (see the supplementary material). The binding affinities were estimated for the MCF-7 cell line as defined above, which complements the previously reported values (Table II). For other cell lines, we used the previously reported data for our simulations (Table II).

Correspondingly, we have considered the respective binding free energy of p53 to p21 and BAX promoter as 1.59 $k_B T$ and 4.6 $k_B T$ inspired from the literature (information presented in Table II), which is qualitatively consistent with the ChIP-seq results that the p21 promoter is bound by p53 threefold stronger than the BAX promoter (supplementary material Figs. S2–S5). A list of concentrations and binding affinity parameters in the model of transcriptional regulation through p53-mediated expression is shown in Table II.

TABLE I. The following references are used for constructing the gene regulatory networks of three cell lines. The arrows ⟶ and ⟞ are used to describe activation and repression in the network.

Cell line	References	Symbol
MCF-7	29 and 77	$p53 \longrightarrow p21$
	29 and 77	$p53 \longrightarrow Bax$
	78	$p53 \longrightarrow p48$
	79	$p53 \longrightarrow PAI$
	27	$p21 \longrightarrow Bax$
	45	$p21 \longrightarrow p48$
K562	80	$p53 \longrightarrow p21$
	80 and 81	$p53 \longrightarrow Bax$
	36	$p53 \longrightarrow p48$
	81 and 82	$p53 \longrightarrow PAI$
	26 and 49	$p21 \dashv Bax$
	36	$p21 \longrightarrow p48$
HCT116	83	$p53 \longrightarrow p21$
	83 and 84	$p53 \longrightarrow Bax$
	85 and 86	$p53 \longrightarrow p48$
	87	$p53 \longrightarrow PAI$
	28 and 88	$p21 \dashv Bax$
	28	$p21 \dashv p48$

TABLE II. Values of parameters used in our calculations. The symbols ε_{p53^*-RE}, $\varepsilon_{p53-RNAP}$, and $\varepsilon_{RNAP-DNA}$ are the parameters for the binding between p53 and response elements (REs) of various genes, $p53^*$ and RNAP; RNAP and DNA, respectively. Symbols λ_{p53^*} and λ_R are the activities for $p53^*$ and RNAP, respectively. $p53^*$ binds to its RE elements in the various genes tightly with dissociation constants (K_D). The experimental p53 ChIP-seq analysis, as presented in the supplementary material, supports the following binding data.

Interaction	Symbol	Value ($k_B T$)	References
$p53^*$-p21 RE	$\varepsilon_{p53^*-RE^{p21}}$	1.59	89 and 90
$p53^*$-BAX RE	$\varepsilon_{p53^*-RE^{BAX}}$	4.6	91 and 89
$p53^*$-p48 RE	$\varepsilon_{p53^*-RE^{p48}}$	3.1	89 and 92
$p53^*$-PAI RE	$\varepsilon_{p53^*-RE^{p48}}$	2.2	89
RNAP-DNA	$\varepsilon_{RNAP-DNA}$	0.69	93
$p53^*$-RNAP	ω_{p53^*-RNAP}	−3	94 and 95
Activities	**Symbol**	**Value(M)**	**References**
p53 activity	λ_{p53^*}	0.13×10^{-6}	96, 97, and 98
RNAP activity	λ_R	9.9×10^{-6}	99

III. RESULTS

Let us consider a cell that undergoes a transition between different states upon binding of p53* to the promoter region of four cell fate-determining genes. We will focus on the importance of the topology of a network of interactions that alter a cell's fate. We rationalized the network topology for different cell lines, MCF-7, HCT116, and K562, which have different gene expression patterns,[27,28,45–48,50] triggering diverse cell fates.

A. Phase transitions associated with cell state transitions

We first aim to identify if there are any phase transitions associated with the binding of p53* to the promoter regions of the genes of interest. We probe two critical questions: (a) Can the binding of p53* push a cell to transition between different states? (b) If it happens, what is the role of the topology of the interaction network for these transitions? We chose the fraction of bound p53* at equilibrium, c^*, as our order parameter to study the phase transition behavior.[59] We further vary the topology parameter, w, which is defined as the average number of edges of the network, to mimic the cellular variation. We calculate w from our grand canonical Monte Carlo (GCMC) simulations for the three different cell lines (w = 2.02, 2.97, and 4.03) as considered in our study. Since the average is taken over the Grand Canonical Monte Carlo (GCMC) simulation run, which generally involves the addition of biomolecules, deletion of biomolecules, or displacement of the biomolecule on the lattice, and is subjected to the Metropolis algorithm, we have six activation/repression possibilities for each cell line, as seen in the network topology. The average value for w represents the occurrence of any particular event (out of six possible activation/repression events) for three different cell lines for a fixed concentration of p53 (e.g., $\lambda_{p53^*} = 130nM$).

We calculate c^* as a function of the initial concentration c_0 of p53*, which is shown in the Fig. 4. We also consider three different cell lines by varying the w parameter in this study. We note an S-shaped curve for each cell line, which is a signature of phase transition exhibited in a cell upon p53* binding. To clarify whether this phase transition is continuous or discontinuous, we calculate the equilibrium free energy of interaction ΔF^* as included in the inset of Fig. 4. This analysis revealed that the system exhibits bistability, showing a signature of first-order phase transitions upon p53 binding.

The concentration of p53* at which the model network exhibits a transition is referred to as the potency point, and the point at which the p53* binding to the promoter saturates is referred to as the efficacy point.[60] We draw a line at the potency point to compare a qualitative signature of these transitions among the three cell lines. They are different, as revealed by our analysis. We note that the potency points for the HCT116, K562, and MCF-7 cell lines are at 2.2, 1.3, and 0.81 μM, showing that HCT116 requires more p53* to saturate the promoter. However, MCF-7 takes the least amount of

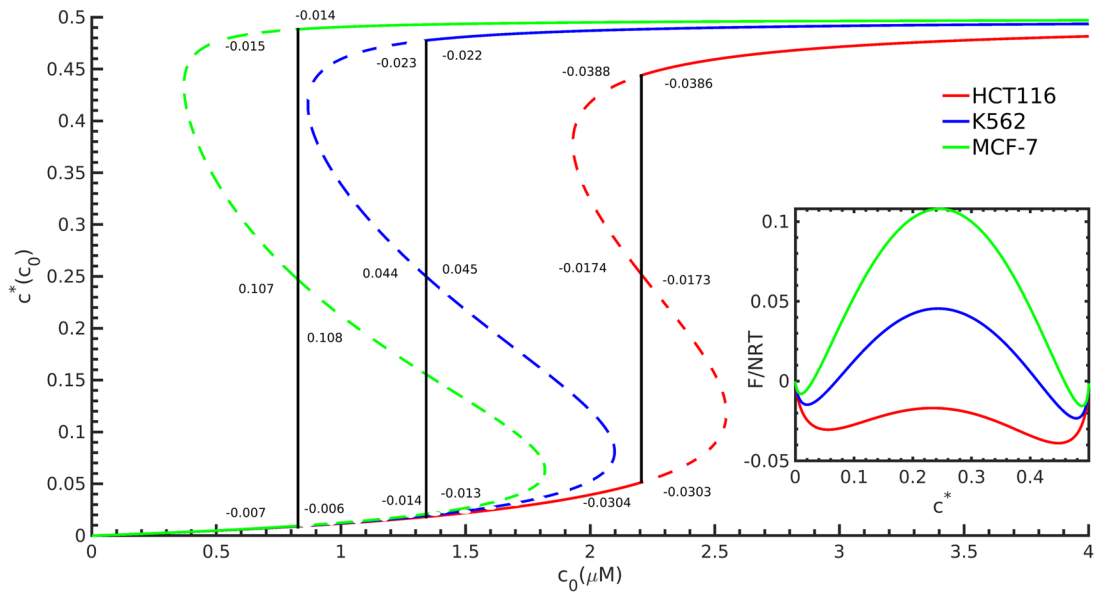

FIG. 4. The binding curves calculated for different cell lines based on their network topology. In our analysis, we set m = 2, taking into account that a p53 tetramer covers about 20 bp upon DNA binding,[24] with two lattice units accounting for symmetric half-sites of the tetramer. Following previous works,[12,56] the free energy value for the nearest neighbor interaction can be estimated as $\varepsilon_1 = -3$RT, and hence, $a_1 = e^{-\frac{\varepsilon_1}{RT}} = e^3$. The energy of phosphorylation of p53 and direct binding of p53 to DNA can be estimated as $\varepsilon_2 = \mu_0 - \varepsilon_0 = -9$RT, and hence, $a_2 = e^{-\frac{\varepsilon_2}{RT}} = e^9$ and $K = e^{-\frac{\mu_0 - \varepsilon_0}{RT}} = e^9$. The connectivity parameters (w) obtained from GCMC simulations for the three cell lines, HCT116, K562, and MCF-7, are 2.02, 2.97, and 4.03, respectively. The binding curves for these cell lines are shown correspondingly in red, blue, and green colors in the main figure and the inset. The dotted lines denote the unstable region obtained from the free energy analysis presented in the inset of the figure. The network topology governing the cell lines influences the first-order transition associated with p53 binding.

p53* to saturate the promoter. We also note that the saturation level can predict gene dependencies in cancer cell lines by altering the gene expression profiles. The origin of differential behavior in these three cell lines' phase transitions primarily arises from the difference in network topology, which we included through the w parameter, as discussed earlier.[52,53,61]

B. The role of network topology

p53 is a crucial transcription factor that determines cellular fate by interacting with the promoter regions of various genes with a wide range of binding affinity. Here, four genes, P21, BAX, P48, and PAI, participate in p53* binding, and the degree of its binding determines a cell's fate.[48,62] The differential expression of these four genes upon binding of p53* is critical to determining whether the cell enters the cell cycle arrest, apoptosis, DNA repair, etc. However, the binding of p53* may be influenced by many other factors, such as (a) internal rewiring of the GRN, (b) interfering with other proteins, and (c) abrupt external perturbation. Since we restrict our study to an isolated GRN within an equilibrium regime, we ignore all other factors except internal rewiring. To demonstrate the importance of the internal network rewiring, we first investigate gene expression changes upon binding p53* to the promoter regions of these four genes in the absence and presence of an arbitrary internal network.

In the following calculation (5), we analyzed the gene response function in the absence of any connectivity between cell fate-determining genes, and we observed that the binding of p53* to genes takes place sequentially as a function of its increasing concentration owing to its wide range of binding affinities. However, we find a significant change in the gene expression pattern when considering a few arbitrary links among these genes in the network. We present the response functions for both cases in Fig. 5. The rationale behind adding different links between these four genes is that they may vary between different cell lines.[17,36,37]

Without connections between the genes, we observe a sequential expression for these genes, but all of them are expressed at the same saturation level at large values of λ_{p53}. In other words, these four genes express differently at low values of λ_{p53}, but their relative expressions are almost identical at large values of λ_{p53}. The differential expression at low values of λ_{p53} appears due to the different binding affinities of the promoter regions of these four genes to the p53*. Therefore, if a cancer cell consists of these four genes without internal links, the cell reaches equiprobably to any of these four states. However, internal links show differential expressions, even at large λ_{p53} values. The results indicate the importance of internal links that determine a differential expression. For example, all four genes express differentially upon introducing two inhibitory loops. Thus, the internal gene networks for different cell lines significantly differ. We discuss this in detail below by considering three different cancer cell lines.

C. Comparison of different cancer cell lines

Human cancer cell lines are widely used in the biology community to understand gene regulation and develop anticancer strategies.[63–65] Since cancer can progress through a p53-dependent pathway,[66] the network of four genes considered here is important for controlling whether the cell enters the cancer state or not.[67] Here, we focus on three cell lines: (a) breast cancer (MCF-7), (b) colorectal cancer (HCT116), and (c) leukemia (K562). The internal links among the four genes of these three cell lines are different, producing qualitatively different gene expressions and determining the cell fate.

We performed partition function-based analysis and Grand Canonical Monte Carlo (GCMC) simulation for each of the networks.[56] The interaction parameters for this simulation are presented in Table II. These parameters are further supported by the ChIP-seq analysis for the genome wide binding of the phosphorylated p53 repressor in the MCF-7 cancer cell line

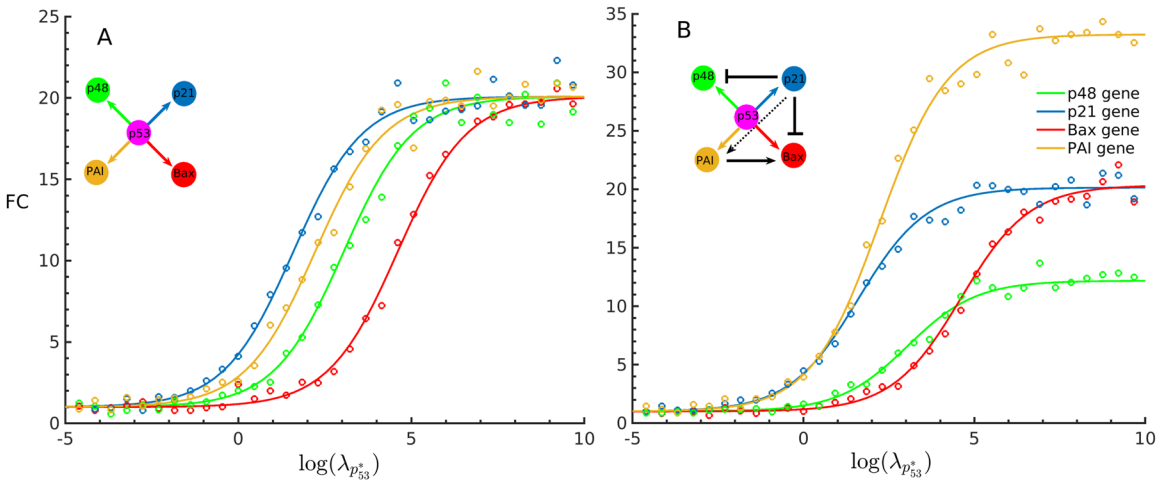

FIG. 5. The expression fold change (FC) for different genes in the absence (a) and presence of internal connectivity (b). The respective networks are shown in the inset of the figure. We have marked response curves for various genes, such as p21, Bax, p48, and PAI, with respective blue, red, green, and yellow colors in the legend for panels (a) and (b). Solid lines correspond to the theoretical predictions, and circles represent the simulation results.

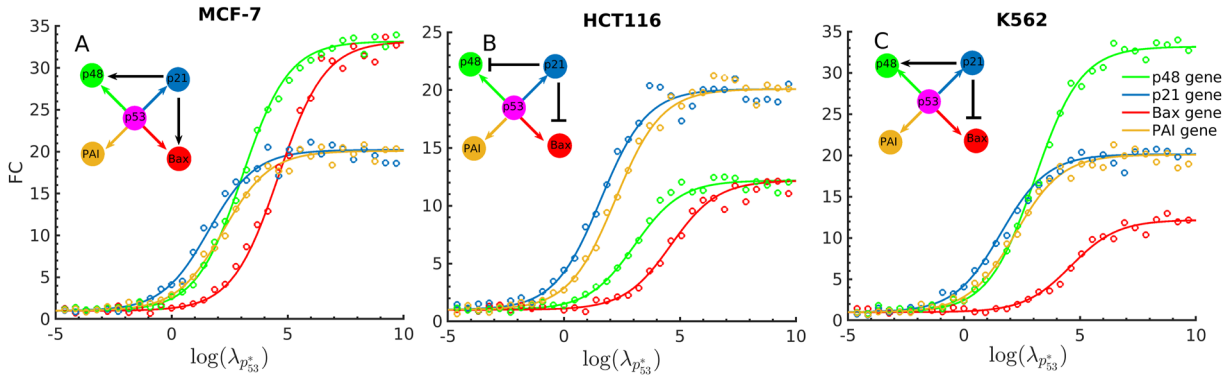

FIG. 6. The expression fold change (FC) of different genes as determined for three different cell lines. Since the internal connectivity among the different genes for the cell lines is different, we show them in the figure. The binding of p53* to the promoter regions of the four genes is heterogeneous and explores the possibility of differential gene expression and the fate of a cell. We have marked response curves for various genes, such as p21, Bax, p48, and PAI with respective blue, red, green, and yellow colors in the legend for panels (a), (b), and (c). Here, the solid lines and circles represent the theoretical results and the simulation results, respectively.

(supplementary material). Our calculations in Fig. 6 show that the connectivity among genes alters gene expression significantly upon binding of p53* to the promoter regions of four cell fate-determining genes. Our analysis reveals that the MCF-7 cell line predominantly expresses p48 and BAX, which either repair DNA or direct it to apoptosis. Both of these mechanisms can inhibit cancer progression.[29,68] We find significantly different gene expressions between the HCT116 and the MCF-7 cell lines. As observed from our analysis, the repression effect of the p21 gene triggers the activation of PAI and p21 genes, which either inhibit angiogenesis or arrest the cell cycle. However, p48 is expressed exclusively in K562 cells, as evident from our analysis. Thus, an underappreciated role of p53* in controlling the expression for the cell fate-determining genes is in modifying the network topology.[62,69]

IV. DISCUSSIONS AND CONCLUSIONS

Transitions between different cell states are governed by binding events at *cis*-regulatory regions, which are affected by 3D genome organization among other factors. A number of previous studies addressed TF binding network construction, other studies built thermodynamic models for TF binding at *cis*-regulatory regions, and a large group of approaches studied the effects of 3D genome organization on TF binding and gene expression. Here, we combine these three different research directions in an attempt to account for both *cis*-regulatory TF binding and long-range mean-field effects of chromatin organization on gene network topology. We applied this idea to minimalist p53 networks.

The core assumptions of our modeling are the following: p53 binds reversibly and site-specifically to promoters of its target genes; p53 can be phosphorylated or not, which determines its regulatory activity; the edges of the network in the form of a pre-selected small number of genes of interest are fixed, but the topology of the network is not fixed and can be different in different cells. As a proof of concept, we consider a minimalist network of four key cell fate genes, but the model is not limited to these genes and can be expanded to a more complete network.

p53 maintains its low level in a healthy cell by a continuous degradation mechanism through an interaction with MDM2.[70] However, DNA damage results in the phosphorylation of p53, which inhibits binding with MDM2, and thus, the concentration of p53* is stabilized.[71] The p53* tetramer controls many cellular processes, including cell fate, i.e., cell cycle arrest, apoptosis, senescence, inhibition of angiogenesis, DNA repair, and metastasis.[48] For example, apoptosis or cell cycle arrest is triggered by activating P21 upon binding tetrameric p53*, which leads to the production of p21. p21 binds with another cyclin-dependent kinase complex (CDK/cyclin) that promotes cell cycle arrest.[21,31] Failing to bind p53* to these cell fate-determining genes promotes human cancer progression. Therefore, it is important to understand the mechanisms behind p53* dependent cellular functionality in cancer onset.[72]

The gene network studied here exhibits multiple layers of control, including phosphorylation of p53 that alters its biological activity and the binding affinity to the promoter regions of the cell-fate-determining genes.[15,17] Here, we investigated the role of p53* in determining the cell fate through the lens of the free energy minimum model. We showed that the binding of p53* to the promoter regions of these genes can promote a phase transition between different cell states. We demonstrated how such transitions occur upon binding phosphorylated p53 at the promoter region of target genes of the core regulatory networks, taking into account long-range chromatin interactions. The transition is discontinuous or first order as revealed by the change in sign of the calculated free energy from our proposed model at equilibrium. The analysis demonstrates that the system exhibits bistability.[59] We further explored the phase transition behavior for different cancer cell lines, MCF-7, HCT116, and K562, as they have the same constituents, but the network topologies differ. Our results reveal that phase transition behavior, which has been studied previously for DNA–ligand systems,[52,53] strongly depends on network topology in the case of TF-DNA binding.

To further pin down the state of the cell, we introduced a grand partition function for the biological networks and performed GCMC

simulations of them to explore the microscopic origin of the cell fate.[73] We found a strong dependence of cell fate on the network topology. For example, the MCF-7 cell line predominantly expresses P48 and BAX, which either repair DNA or follow apoptosis. However, P21 represses P48 and BAX genes in HCT116 cells, ultimately activating P21 and PAI genes, inhibiting angiogenesis, or arresting the cell cycle. On the other hand, P48 expression exclusively promotes DNA repair in the K562 cell line. Therefore, the diverse range of outcomes obtained from the different cell lines governed by the network topology provides a better understanding of the actual state of the cell.[69,74]

The cell phenotype is often the result of the action of few key transcription factors that regulate the expression and are inherently linked with the cascading event of the cell fate decisions.[75] The tetrameric p53* plays a key role in activating some of many genes based on the sequence-specific response elements.[76] A prime question in this regard is how p53 decides the cellular fate based on a wide range of binding affinity dependent on the promoters and internal networks for the cell fate-determining genes. In this work, we investigated multiple biophysical processes and gene networks to understand the fine-tuned expression and cell fate. Our modeling established a computational framework that can be employed to furnish transcription patterns for vast possibilities of cellular fates. Our analyses for the different cell lines were based on the network topologies known from the literature. However, there is a possibility that some other factors can dominate over network topology, such as the entanglement of these genes in 3D space, dysregulated transcriptional programs that result from genetic mutations, epigenetic regulation, RNA stability, protein translation, and post-translational control. Our proposed theoretical method could include those factors in the model, which we are currently exploring.

SUPPLEMENTARY MATERIAL

See the supplementary material for visualization of a ChIP-seq dataset with p53 binding in MCF-7 cells in the UCSC Genome Browser.

ACKNOWLEDGMENTS

P.G. acknowledges the financial support from UGC. S.K.S. is supported by SERB, Department of Science and Technology, Government of India (Grant Nos. MTR/2020/000553 and CRG/2022/000345). V.T. was supported by Cancer Research UK Grant Nos. EDDPMA-Nov21/100044 and SEBPCTA-2022/100001 and BBSRC Grant No. BB/X511171/1.

AUTHOR DECLARATIONS

Conflict of Interest

The authors have no conflicts to disclose.

Author Contributions

Pankaj Gautam: Conceptualization (equal); Data curation (equal); Formal analysis (equal); Investigation (equal); Methodology (equal); Software (equal); Validation (equal); Visualization (equal); Writing – original draft (equal); Writing – review & editing (equal). **Isabella Ciuta**: Investigation (equal); Visualization (equal); Writing – review & editing (equal). **Vladimir B. Teif**: Conceptualization (equal); Funding acquisition (equal); Investigation (equal); Methodology (equal); Supervision (equal); Writing – review & editing (equal). **Sudipta Kumar Sinha**: Conceptualization (equal); Formal analysis (equal); Funding acquisition (equal); Investigation (equal); Methodology (equal); Project administration (equal); Resources (equal); Supervision (equal); Writing – original draft (equal); Writing – review & editing (equal).

DATA AVAILABILITY

Data and relevant code for these analyses are available at https://zenodo.org/records/10042982.

REFERENCES

[1] P. E. Wright and H. J. Dyson, "Intrinsically disordered proteins in cellular signalling and regulation," Nat. Rev. Mol. Cell Biol. **16**, 18–29 (2015).
[2] K. D. Sullivan, M. D. Galbraith, Z. Andrysik, and J. M. Espinosa, "Mechanisms of transcriptional regulation by p53," Cell Death Differ. **25**, 133–143 (2018).
[3] A. J. Levine, "p53, the cellular gatekeeper for growth and division," Cell **88**, 323–331 (1997).
[4] K. T. Bieging, S. S. Mello, and L. D. Attardi, "Unravelling mechanisms of p53-mediated tumour suppression," Nat. Rev. Cancer **14**, 359–370 (2014).
[5] M. H. Kubbutat, S. N. Jones, and K. H. Vousden, "Regulation of p53 stability by Mdm2," Nature **387**, 299–303 (1997).
[6] Y. Haupt, R. Maya, A. Kazaz, and M. Oren, "Mdm2 promotes the rapid degradation of p53," Nature **387**, 296–299 (1997).
[7] A. M. Bode and Z. Dong, "Post-translational modification of p53 in tumorigenesis," Nat. Rev. Cancer **4**, 793–805 (2004).
[8] K. H. Vousden and C. Prives, "Blinded by the light: The growing complexity of p53," Cell **137**, 413–431 (2009).
[9] F. Serra, A. Nieto-Aliseda, L. Fanlo-Escudero, L. Rovirosa, M. Cabrera-Pasadas, A. Lazarenkov, B. Urmeneta, A. Alcalde-Merino, E. M. Nola, A. L. Okorokov *et al.*, "p53 rapidly restructures 3D chromatin organization to trigger a transcriptional response," Nat. Commun. **15**, 2821 (2024).
[10] A. Garg, G. Kumar, V. Singh, and S. Sinha, "Doxorubicin catalyses self-assembly of p53 by phase separation," Curr. Res. Struct. Biol. **7**, 100133 (2024).
[11] D. Datta, A. Navalkar, A. Sakunthala, A. Paul, K. Patel, S. Masurkar, L. Gadhe, S. Sengupta, M. Poudyal, J. Devi, A. S. Sawner, P. Kadu, R. Shaw, S. Pandey, S. Mukherjee, N. Gahlot, K. Sengupta, and S. K. Maji, "Nucleo-cytoplasmic environment modulates spatio-temporal p53 phase separation," bioRxiv:10.1101/2023.10.16.562512 (2023).
[12] C. W. Lee, J. C. Ferreon, A. C. M. Ferreon, M. Arai, and P. E. Wright, "Graded enhancement of p53 binding to CREB-binding protein (CBP) by multisite phosphorylation," Proc. Natl. Acad. Sci. U. S. A. **107**, 19290–19295 (2010).
[13] J. C. Ferreon, C. W. Lee, M. Arai, M. A. Martinez-Yamout, H. J. Dyson, and P. E. Wright, "Cooperative regulation of p53 by modulation of ternary complex formation with CBP/p300 and HDM2," Proc. Natl. Acad. Sci. U. S. A. **106**, 6591–6596 (2009).
[14] A. Olsson, C. Manzl, A. Strasser, and A. Villunger, "How important are post-translational modifications in p53 for selectivity in target-gene transcription and tumour suppression?," Cell Death Differ. **14**, 1561–1575 (2007).
[15] C. Chao, D. Herr, J. Chun, and Y. Xu, "Ser18 and 23 phosphorylation is required for p53-dependent apoptosis and tumor suppression," EMBO J. **25**, 2615–2622 (2006).
[16] A. Gatti, H.-H. Li, J. A. Traugh, and X. Liu, "Phosphorylation of human p53 on Thr-55," Biochemistry **39**, 9837–9842 (2000).
[17] L. D. Mayo, Y. R. Seo, M. W. Jackson, M. L. Smith, J. R. Guzman, C. K. Korgaonkar, and D. B. Donner, "Phosphorylation of human p53 at serine 46

determines promoter selection and whether apoptosis is attenuated or amplified," J. Biol. Chem. **280**, 25953–25959 (2005).
[18]J. Loughery, M. Cox, L. M. Smith, and D. W. Meek, "Critical role for p53-serine 15 phosphorylation in stimulating transactivation at p53-responsive promoters," Nucleic Acids Res. **42**, 7666–7680 (2014).
[19]A. J. Levine and M. Oren, "The first 30 years of p53: Growing ever more complex," Nat. Rev. Cancer **9**, 749–758 (2009).
[20]E. R. Kastenhuber and S. W. Lowe, "Putting p53 in context," Cell **170**, 1062–1078 (2017).
[21]S. Rokudai, Y. Aikawa, Y. Tagata, N. Tsuchida, Y. Taya, and I. Kitabayashi, "Monocytic leukemia zinc finger (MOZ) interacts with p53 to induce p21 expression and cell-cycle arrest," J. Biol. Chem. **284**, 237–244 (2009).
[22]A. B. Williams and B. Schumacher, "p53 in the DNA-damage-repair process," Cold Spring Harbor Perspect. Med. **6**, a026070 (2016).
[23]J. G. Teodoro, A. E. Parker, X. Zhu, and M. R. Green, "p53-mediated inhibition of angiogenesis through up-regulation of a collagen prolyl hydroxylase," Science **313**, 968–971 (2006).
[24]M. Farkas, H. Hashimoto, Y. Bi, R. V. Davuluri, L. Resnick-Silverman, J. J. Manfredi, E. W. Debler, and S. B. McMahon, "Distinct mechanisms control genome recognition by p53 at its target genes linked to different cell fates," Nat. Commun. **12**, 484 (2021).
[25]K.-W. Choi, H. Suh, H. L. Oh, C. Ryou, and C.-H. Lee, "p21CIP1 induces apoptosis via binding to BCL2 in lncap prostate cancer cells treated with MCS-C3, a novel carbocyclic analog of pyrrolopyrimidine," Anticancer Res. **36**, 213–220 (2016).
[26]R. Rodriguez and M. Meuth, "Chk1 and p21 cooperate to prevent apoptosis during DNA replication fork stress," Mol. Biol. Cell **17**, 402–412 (2006).
[27]Y. S. Tor, L. S. Yazan, J. B. Foo, A. Wibowo, N. Ismail, Y. K. Cheah, R. Abdullah, M. Ismail, I. S. Ismail, and S. K. Yeap, "Induction of apoptosis in MCF-7 cells via oxidative stress generation, mitochondria-dependent and caspase-independent pathway by ethyl acetate extract of dillenia suffruticosa and its chemical profile," PLoS One **10**, e0127441 (2015).
[28]A. G. Georgakilas, O. A. Martin, and W. M. Bonner, "p21: A two-faced genome guardian," Trends Mol. Med. **23**, 310–319 (2017).
[29]N. B. Alitheen, S. K. Yeap, M. N. Akhtar, K. L. Lim, N. Abu, W. Y. Ho, S. Zareen, K. Rohani, H. Ky, S. W. Tan, and N. Lajis, "Synthesis of an anthraquinone derivative (DHAQC) and its effect on induction of G2/M arrest and apoptosis in breast cancer MCF-7 cell line," Drug Des., Dev. Ther. **2015**, 983–992.
[30]L. D. Attardi, S. W. Lowe, J. Brugarolas, and T. Jacks, "Transcriptional activation by p53, but not induction of the p21 gene, is essential for oncogene-mediated apoptosis," EMBO J. **15**, 3693–3701 (1996).
[31]N. Bissonnette and D. Hunting, "p21-induced cycle arrest in G1 protects cells from apoptosis induced by UV-irradiation or RNA polymerase II blockage," Oncogene **16**, 3461–3469 (1998).
[32]K. F. Macleod, N. Sherry, G. Hannon, D. Beach, T. Tokino, K. Kinzler, B. Vogelstein, and T. Jacks, "p53-dependent and independent expression of p21 during cell growth, differentiation, and DNA damage," Genes Dev. **9**, 935–944 (1995).
[33]T. Furuta, R. Hayward, L. Meng, H. Takemura, G. Aune, W. Bonner, M. Aladjem, K. Kohn, and Y. Pommier, "p21CDKN1A allows the repair of replication-mediated DNA double-strand breaks induced by topoisomerase I and is inactivated by the checkpoint kinase inhibitor 7-hydroxystaurosporine," Oncogene **25**, 2839–2849 (2006).
[34]S. Kuljaca, T. Liu, T. Dwarte, M. Kavallaris, M. Haber, M. D. Norris, J. Martin-Caballero, and G. M. Marshall, "The cyclin-dependent kinase inhibitor, p21 WAF1, promotes angiogenesis by repressing gene transcription of thioredoxin-binding protein 2 in cancer cells," Carcinogenesis **30**, 1865–1871 (2009).
[35]Y. Chen, R. J. Kelm, Jr., R. C. Budd, B. E. Sobel, and D. J. Schneider, "Inhibition of apoptosis and caspase-3 in vascular smooth muscle cells by plasminogen activator inhibitor type-1," J. Cell. Biochem. **92**, 178–188 (2004).
[36]Z. Fan, H. Luo, J. Zhou, F. Wang, W. Zhang, J. Wang, S. Li, Q. Lai, Y. Xu, G. Wang *et al.*, "Checkpoint kinase-1 inhibition and etoposide exhibit a strong synergistic anticancer effect on chronic myeloid leukemia cell line K562 by impairing homologous recombination DNA damage repair," Oncol. Rep. **44**, 2152–2164 (2020).
[37]R. Mirzayans, B. Andrais, A. Scott, Y. W. Wang, R. H. Weiss, and D. Murray, "Spontaneous γH2AX foci in human solid tumor-derived cell lines in relation to p21WAF1 and WIP1 expression," Int. J. Mol. Sci. **16**, 11609–11628 (2015).
[38]A. W. Braithwaite, J. A. Royds, and P. Jackson, "The p53 story: Layers of complexity," Carcinogenesis **26**, 1161–1169 (2005).
[39]M. Lavin and N. Gueven, "The complexity of p53 stabilization and activation," Cell Death Differ. **13**, 941–950 (2006).
[40]G. Lahav, N. Rosenfeld, A. Sigal, N. Geva-Zatorsky, A. J. Levine, M. B. Elowitz, and U. Alon, "Dynamics of the p53-MDM2 feedback loop in individual cells," Nat. Genet. **36**, 147–150 (2004).
[41]S.-Y. Shieh, M. Ikeda, Y. Taya, and C. Prives, "DNA damage-induced phosphorylation of p53 alleviates inhibition by MDM2," Cell **91**, 325–334 (1997).
[42]L. T. Vassilev, B. T. Vu, B. Graves, D. Carvajal, F. Podlaski, Z. Filipovic, N. Kong, U. Kammlott, C. Lukacs, C. Klein *et al.*, "In vivo activation of the p53 pathway by small-molecule antagonists of MDM2," Science **303**, 844–848 (2004).
[43]C. Tovar, J. Rosinski, Z. Filipovic, B. Higgins, K. Kolinsky, H. Hilton, X. Zhao, B. T. Vu, W. Qing, K. Packman *et al.*, "Small-molecule MDM2 antagonists reveal aberrant p53 signaling in cancer: Implications for therapy," Proc. Natl. Acad. Sci. U. S. A. **103**, 1888–1893 (2006).
[44]A. Saramäki, C. M. Banwell, M. J. Campbell, and C. Carlberg, "Regulation of the human p21 (waf1/cip1) gene promoter via multiple binding sites for p53 and the vitamin D_3 receptor," Nucleic Acids Res. **34**, 543–554 (2006).
[45]Y. He, Z. Wang, Y. Hu, X. Yi, L. Wu, Z. Cao, and J. Wang, "Sensitive and selective monitoring of the DNA damage-induced intracellular p21 protein and unraveling the role of the p21 protein in DNA repair and cell apoptosis by surface plasmon resonance," Analyst **145**, 3697–3704 (2020).
[46]H. Ehrhardt, S. Pfeiffer, D. Schrembs, F. Wachter, M. Grunert, and I. Jeremias, "Activation of DNA damage response by antitumor therapy counteracts the activity of vinca alkaloids," Anticancer Res. **33**, 5273–5287 (2013).
[47]J.-H. Yen, C.-Y. Lin, C.-H. Chuang, H.-K. Chin, M.-J. Wu, and P.-Y. Chen, "Nobiletin promotes megakaryocytic differentiation through the MAPK/ERK-dependent EGR1 expression and exerts anti-leukemic effects in human chronic myeloid leukemia (CML) K562 cells," Cells **9**, 877 (2020).
[48]S. L. Harris and A. J. Levine, "The p53 pathway: Positive and negative feedback loops," Oncogene **24**, 2899–2908 (2005).
[49]R.-F. Li, Y.-Q. Feng, J.-H. Chen, L.-T. Ge, S.-Y. Xiao, and X.-L. Zuo, "Naringenin suppresses K562 human leukemia cell proliferation and ameliorates adriamycin-induced oxidative damage in polymorphonuclear leukocytes," Exp. Ther. Med. **9**, 697–706 (2015).
[50]C. Drullion, C. Trégoat, V. Lagarde, S. Tan, R. Gioia, M. Priault, M. Djavaheri-Mergny, A. Brisson, P. Auberger, F. Mahon, and J. M. Pasquet, "Apoptosis and autophagy have opposite roles on imatinib-induced K562 leukemia cell senescence," Cell Death Dis. **3**, e373 (2012).
[51]S. Ranganathan, D. Halagowder, and N. D. Sivasithambaram, "Quercetin suppresses twist to induce apoptosis in MCF-7 breast cancer cells," PLoS One **10**, e0141370 (2015).
[52]V. B. Teif, S. G. Haroutiunian, V. I. Vorob'ev, D. Y. Lando, and V. Ivanov, "Short-range interactions and size of ligands bound to dna strongly influence adsorptive phase transition caused by long-range interactions," J. Biomol. Struct. Dyn. **19**, 1093–1100 (2002).
[53]D. Y. Lando and V. B. Teif, "Long-range interactions between ligands bound to a DNA molecule give rise to adsorption with the character of phase transition of the first kind," J. Biomol. Struct. Dyn. **17**, 903–911 (2000).
[54]G. Scatchard, "The attractions of proteins for small molecules and ions," Ann. N. Y. Acad. Sci. **51**, 660–672 (1949).
[55]V. B. Teif, F. Erdel, D. A. Beshnova, Y. Vainshtein, J.-P. Mallm, and K. Rippe, "Taking into account nucleosomes for predicting gene expression," Methods **62**, 26–38 (2013), part of Special Issue: Modeling Gene Expression.
[56]P. Gautam and S. Kumar Sinha, "Anticipating response function in gene regulatory networks," J. R. Soc., Interface **18**, 20210206 (2021).
[57]P. Gautam and S. K. Sinha, "Theoretical investigation of functional responses of bio-molecular assembly networks," Soft Matter **19**, 3803–3817 (2023).
[58]P. Gautam and S. K. Sinha, "The blueprint of logical decisions in a NF-κB signaling system," ACS Omega **9**, 22625–22634 (2024).
[59]H. B. Callen, *Thermodynamics and an Introduction to Thermostatistics* (John Wiley & Sons, 1991).

[60]C. P. Martins, L. Brown-Swigart, and G. I. Evan, "Modeling the therapeutic efficacy of p53 restoration in tumors," Cell **127**, 1323–1334 (2006).
[61]V. B. Teif, "Ligand-induced DNA condensation: Choosing the model," Biophys. J. **89**, 2574–2587 (2005).
[62]A. Hafner, M. L. Bulyk, A. Jambhekar, and G. Lahav, "The multiple mechanisms that regulate p53 activity and cell fate," Nat. Rev. Mol. Cell Biol. **20**, 199–210 (2019).
[63]I. Cortes-Ciriano, G. J. Van Westen, G. Bouvier, M. Nilges, J. P. Overington, A. Bender, and T. E. Malliavin, "Improved large-scale prediction of growth inhibition patterns using the NCI60 cancer cell line panel," Bioinformatics **32**, 85–95 (2016).
[64]N. M. Abdullah, G. R. Rosania, and K. Shedden, "Selective targeting of tumorigenic cancer cell lines by microtubule inhibitors," PLoS One **4**, e4470 (2009).
[65]P. Guo, J. Yang, D. Liu, L. Huang, G. Fell, J. Huang, M. A. Moses, and D. T. Auguste, "Dual complementary liposomes inhibit triple-negative breast tumor progression and metastasis," Sci. Adv. **5**, eaav5010 (2019).
[66]E. Powell, D. Piwnica-Worms, and H. Piwnica-Worms, "Contribution of p53 to metastasis," Cancer Discovery **4**, 405–414 (2014).
[67]A. Pryczynicz, M. Gryko, K. Niewiarowska, D. Cepowicz, M. Ustymowicz, A. Kemona, and K. Guzińska-Ustymowicz, "Bax protein may influence the invasion of colorectal cancer," World J. Gastroenterol. **20**, 1305 (2014).
[68]R. Cuella-Martin, C. Oliveira, H. E. Lockstone, S. Snellenberg, N. Grolmusova, and J. R. Chapman, "53BP1 integrates DNA repair and p53-dependent cell fate decisions via distinct mechanisms," Mol. Cell **64**, 51–64 (2016).
[69]G. Benstead-Hume, S. K. Wooller, J. Renaut, S. Dias, L. Woodbine, A. M. Carr, and F. M. Pearl, "Biological network topology features predict gene dependencies in cancer cell-lines," Bioinform. Adv. **2**, vbac084 (2022).
[70]D. Alarcon-Vargas and Z. Ronai, "p53–MDM2—The affair that never ends," Carcinogenesis **23**, 541–547 (2002).
[71]N. H. Chehab, A. Malikzay, E. S. Stavridi, and T. D. Halazonetis, "Phosphorylation of SER-20 mediates stabilization of human p53 in response to DNA damage," Proc. Natl. Acad. Sci. U. S. A. **96**, 13777–13782 (1999).
[72]H. E. Marei, A. Althani, N. Afifi, A. Hasan, T. Caceci, G. Pozzoli, A. Morrione, A. Giordano, and C. Cenciarelli, "p53 signaling in cancer progression and therapy," Cancer Cell Int. **21**, 703 (2021).
[73]T. L. Hill, *An Introduction to Statistical Thermodynamics* (Courier Corporation, 1986).
[74]M. Rashid, K. Hari, J. Thampi, N. K. Santhosh, and M. K. Jolly, "Network topology metrics explaining enrichment of hybrid epithelial/mesenchymal phenotypes in metastasis," PLoS Comput. Biol. **18**, e1010687 (2022).
[75]D. Jia, M. K. Jolly, P. Kulkarni, and H. Levine, "Phenotypic plasticity and cell fate decisions in cancer: Insights from dynamical systems theory," Cancers **9**, 70 (2017).
[76]S. E. Kern, K. W. Kinzler, A. Bruskin, D. Jarosz, P. Friedman, C. Prives, and B. Vogelstein, "Identification of p53 as a sequence-specific DNA-binding protein," Science **252**, 1708–1711 (1991).
[77]L. Meng, K. Kohn, and Y. Pommier, "Dose–response transition from cell cycle arrest to apoptosis with selective degradation of Mdm2 and $p21^{waf1/cip1}$ in response to the novel anticancer agent, aminoflavone (NSC 686288)," Oncogene **26**, 4806–4816 (2007).
[78]M. Fischer, "Census and evaluation of p53 target genes," Oncogene **36**, 3943–3956 (2017).
[79]D. J. Elzi, Y. Lai, M. Song, K. Hakala, S. T. Weintraub, and Y. Shiio, "Plasminogen activator inhibitor 1 - insulin-like growth factor binding protein 3 cascade regulates stress-induced senescence," Proc. Natl. Acad. Sci. U. S. A. **109**, 12052–12057 (2012).
[80]E. Mutlu Altundağ, A. M. Yılmaz, B. S. Serdar, A. T. Jannuzzi, S. Koçtürk, and A. S. Yalçın, "Synergistic induction of apoptosis by quercetin and curcumin in chronic myeloid leukemia (K562) cells: II. Signal transduction pathways involved," Nutr. Cancer **73**, 703–712 (2021).
[81]S. Debnath, S. Karan, M. Debnath, J. Dash, and T. K. Chatterjee, "Poly-L-Lysine inhibits tumor angiogenesis and induces apoptosis in ehrlich ascites carcinoma and in sarcoma S-180 tumor," Asian Pac. J. Cancer Prev. **18**, 2255 (2017).
[82]P. A. Apostolidis, S. Lindsey, W. M. Miller, and E. T. Papoutsakis, "Proposed megakaryocytic regulon of p53: The genes engaged to control cell cycle and apoptosis during megakaryocytic differentiation," Physiol. Genomics **44**, 638–650 (2012).
[83]V. S. Thakur, A. Ruhul Amin, R. K. Paul, K. Gupta, K. Hastak, M. K. Agarwal, M. W. Jackson, D. N. Wald, H. Mukhtar, and M. L. Agarwal, "p53-dependent p21-mediated growth arrest pre-empts and protects HCT116 cells from puma-mediated apoptosis induced by EGCG," Cancer Lett. **296**, 225–232 (2010).
[84]P. Ray, D. Guha, J. Chakraborty, S. Banerjee, A. Adhikary, S. Chakraborty, T. Das, and G. Sa, "Crocetin exploits p53-induced death domain (PIDD) and FAS-associated death domain (FADD) proteins to induce apoptosis in colorectal cancer," Sci. Rep. **6**, 32979 (2016).
[85]H.-L. Tsai, Y.-C. Tsai, Y.-C. Chen, C.-W. Huang, P.-J. Chen, C.-C. Li, W.-C. Su, T.-K. Chang, Y.-S. Yeh, T.-C. Yin, and J. Y. Wang, "Microrna-148a induces apoptosis and prevents angiogenesis with bevacizumab in colon cancer through direct inhibition of ROCK1/c-Met via HIF-1α under hypoxia," Aging **14**, 6668 (2022).
[86]A. Sermeus and C. Michiels, "Reciprocal influence of the p53 and the hypoxic pathways," Cell Death Dis. **2**, e164 (2011).
[87]R. Ravi, B. Mookerjee, Z. M. Bhujwalla, C. H. Sutter, D. Artemov, Q. Zeng, L. E. Dillehay, A. Madan, G. L. Semenza, and A. Bedi, "Regulation of tumor angiogenesis by p53-induced degradation of hypoxia-inducible factor 1α," Genes Dev. **14**, 34–44 (2000).
[88]Z. Han, W. Wei, S. Dunaway, J. W. Darnowski, P. Calabresi, J. Sedivy, E. A. Hendrickson, K. V. Balan, P. Pantazis, and J. H. Wyche, "Role of p21 in apoptosis and senescence of human colon cancer cells treated with camptothecin," J. Biol. Chem. **277**, 17154–17160 (2002).
[89]R. L. Weinberg, D. B. Veprintsev, M. Bycroft, and A. R. Fersht, "Comparative binding of p53 to its promoter and DNA recognition elements," J. Mol. Biol. **348**, 589–596 (2005).
[90]X. Sun, H. J. Dyson, and P. E. Wright, "A phosphorylation-dependent switch in the disordered p53 transactivation domain regulates dna binding," Proc. Natl. Acad. Sci. U. S. A. **118**, e2021456118 (2021).
[91]S. Rajagopalan, F. Huang, and A. R. Fersht, "Single-molecule characterization of oligomerization kinetics and equilibria of the tumor suppressor p53," Nucleic Acids Res. **39**, 2294–2303 (2011).
[92]T. Tan and G. Chu, "p53 binds and activates the xeroderma pigmentosum DDB2 gene in humans but not mice," Mol. Cell. Biol. **22**, 3247–3254 (2002).
[93]P. Di Lello, L. M. Miller Jenkins, C. Mas, C. Langlois, E. Malitskaya, A. Fradet-Turcotte, J. Archambault, P. Legault, and J. G. Omichinski, "p53 and tfiiea share a common binding site on the TFB1/p62 subunit of tfiih," Proc. Natl. Acad. Sci. U. S. A. **105**, 106–111 (2008).
[94]N. E. Buchler, U. Gerland, and T. Hwa, "On schemes of combinatorial transcription logic," Proc. Natl. Acad. Sci. U. S. A. **100**, 5136–5141 (2003).
[95]S. K. Singh, Z. Qiao, L. Song, V. Jani, W. Rice, E. Eng, R. A. Coleman, and W.-L. Liu, "Structural visualization of the p53/RNA polymerase II assembly," Genes Dev. **30**, 2527–2537 (2016).
[96]G. Gaglia, Y. Guan, J. V. Shah, and G. Lahav, "Activation and control of p53 tetramerization in individual living cells," Proc. Natl. Acad. Sci. U. S. A. **110**, 15497–15501 (2013).
[97]P. V. Nikolova, J. Henckel, D. P. Lane, and A. R. Fersht, "Semirational design of active tumor suppressor p53 dna binding domain with enhanced stability," Proc. Natl. Acad. Sci. U. S. A. **95**, 14675–14680 (1998).
[98]V. Lloyd, M. Morse, B. Purakal, J. Parker, P. Benard, M. Crone, S. Pfiffner, M. Szmyd, and S. Dinda, "Hormone-like effects of bisphenol a on p53 and estrogen receptor alpha in breast cancer cells," BioRes. Open Access **8**, 169–184 (2019).
[99]H. Meka, F. Werner, S. C. Cordell, S. Onesti, and P. Brick, "Crystal structure and RNA binding of the RPB4/RPB7 subunits of human RNA polymerase II," Nucleic Acids Res. **33**, 6435–6444 (2005).